Dioxygen Activation at Monovalent Nickel

MATTHEW T. KIEBER-EMMONS AND CHARLES G. RIORDAN*

Department of Chemistry and Biochemistry, University of Delaware, Newark, Delaware 19716

Received February 23, 2007

ABSTRACT

The monovalent oxidation state of nickel has received a growing amount of attention in recent years, in part due to its suggested catalytic role in a number of metalloprotein-mediated transformations. In coordination chemistry, nickel(I) is suitable for reductive activation of dioxygen, provided ligands are used that stabilize this less common oxidation state against disproportionation reactions. Two distinct molecular systems have been explored, which have provided access to new nickel–dioxygen structure types, namely, monomeric side-on and end-on superoxo and trans-μ-1,2-peroxo–dinickel complexes. The geometric and electronic structures of the complexes have been established by advanced spectroscopic methods, including resonance Raman and X-ray absorption spectroscopies, and augmented by density functional theory analyses.

Background and Significance

Metal-mediated dioxygen activation continues to fascinate and inspire chemists and biologists due to its practical importance in industrial and biological oxidation reactions.[1] Inspiration comes from a myriad of sources, biology foremost among them. Enzymes, in particular the ubiquitous cytochrome P450 family,[2] have evolved into what are in effect Nature's Fenton reagents, with additional levels of sophistication leading to impressive regio- and chemoselectivity. The two most essential features differentiating enzymatic oxidation catalysis from Fenton chemistry are utilization of the terrestrial pool of dioxygen rather then the corresponding reduced forms (i.e., superoxides and peroxides) and the ability to abrogate toxic radical formation. These attributes allow enzymatic catalysis to achieve a remarkable degree of control during function beyond that available from synthetic systems.

Examination of synthetic systems that activate dioxygen has focused on copper and iron complexes due to the prevalence of these first-row metal ions in enzymes that bind and activate (mono- and dioxygenases) dioxygen.[3] An extensive range of structure types and patterns of reactivity have been defined over the past two decades. In contrast, Nature predominantly sequesters nickel for reactions that involve transformation of one-carbon substrates most essential to early life, i.e., CO, CO_2, and methyl equivalents in anoxic environments.[4] In particular, acetyl coenzyme A synthase,[5] carbon monoxide dehydrogenase,[6] and methyl coenzyme M reductase[7] are the nickel proteins found in anaerobic organisms that catalyze reactions required for autotrophic growth. It is intriguing to consider why Nature has neglected nickel for aerobic oxidation catalysis, given its significant bioavailability and in light of the fact that heavier group-ten congeners have demonstrated synthetic utility in this regard. However, recent biological stimulus for nickel dioxygen chemistry stems from the discovery of two nickel-dependent enzymes that utilize dioxygen and its reduced form, superoxide, in catalysis. Nickel superoxide dismutases (SOD) have been found in several Actinomycetes[8–10] and homologous proteins from cyanobacteria.[11] The SODs catalyze the disproportionation of superoxide to hydrogen peroxide and dioxygen. Half of the reaction is equivalent to the microscopic reverse of dioxygen activation. A novel aspect of the Ni SOD active site is the presence of Cys ligation, residues not previously found at the active site of SODs, presumably because of their oxidative propensity.[12] The mechanism is proposed to entail inner sphere superoxide ligation and dismutation via the $Ni^{3+/2+}$ redox couple.[13–15] Also of relevance in this context is the occurrence of a nickel dioxygenase.[16] The mononuclear enzyme from *Klebsiella pneumoniae* catalyzes oxidative C–C bond rupture of acireductone, generating formic acid, CO, and methylthiopropionate.[17] The metal likely serves as a Lewis acid, binding the *cis*-β-keto-enolate substrate, activating it for direct attack by O_2.[18] Thus, Ni–O_2 intermediates and Ni-based redox processes are not involved in catalysis, a hypothesis verified in model studies.[19]

While nickel complexes are generally inert to dioxygen, the metal's supporting ligand can engender such reactivity. Highly electron rich ligands bound to Ni^{2+} reduce the $Ni^{3+/2+}$ redox potential so that the oxidation reaction becomes thermodynamically favored. For example, nickel–peptide complexes, in which main chain amides ligate the metal, are readily oxidized to Ni^{3+}.[20] Similarly, certain Ni^{2+}–thiolate complexes are susceptible to sulfur oxidation, yielding sulfoxides, sulfones, and sulfonates.[21] Directing the strong oxidants generated upon reaction with O_2 toward exogenous substrates remains a significant challenge,[22,23] in large part because of the kinetic preference for ligand oxidation.[24,25]

In light of the chemistry emerging from nickel–oxygen species, synthetic strategies aimed at discovery of new nickel–dioxygen structure types have received renewed attention. The most common approach involves the use of hydrogen peroxide and Ni^{2+} salts (Figure 1). For example, Hikichi and co-workers were able to prepare the first bis-μ-oxo–dinickel complex by reaction of $[(Tp^*)Ni]_2(\mu\text{-}OH)_2$ with hydrogen peroxide.[26] Similarly, Shiren and co-workers

Matthew T. Kieber-Emmons was born in 1980 in Buffalo, NY, the second of four siblings. He attended Saint Joseph's University in Philadelphia, home of the legendary Hawk basketball team, and worked under the direction of B. S. Hammes, graduating in 2002. He is currently pursuing graduate studies at the University of Delaware.

Charles G. Riordan was born in 1964 in New York, NY, and raised in Connecticut. He received a B.A. in 1986 from the College of the Holy Cross (with R. S. Herrick) and his Ph.D. in 1990 from Texas A&M University with M. Y. Darensbourg and served as a postdoctoral associate at the University of Chicago with J. Halpern. He is currently Professor of Chemistry and Biochemistry at the University of Delaware.

* Corresponding author.

10.1021/ar700043n CCC: $37.00
Published on Web 05/23/2007

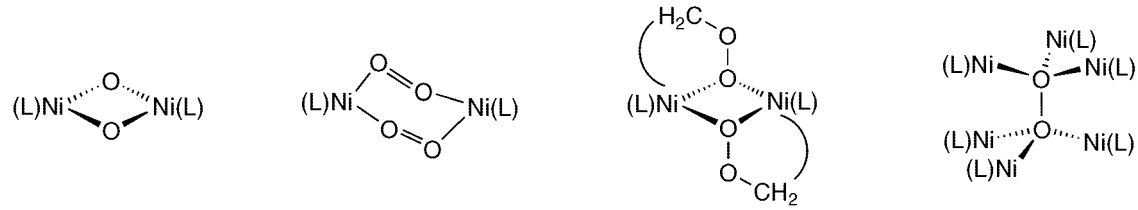

FIGURE 1. Previous Ni–O_x structure types derived from Ni^{2+} salts and H_2O_2.

Scheme 1

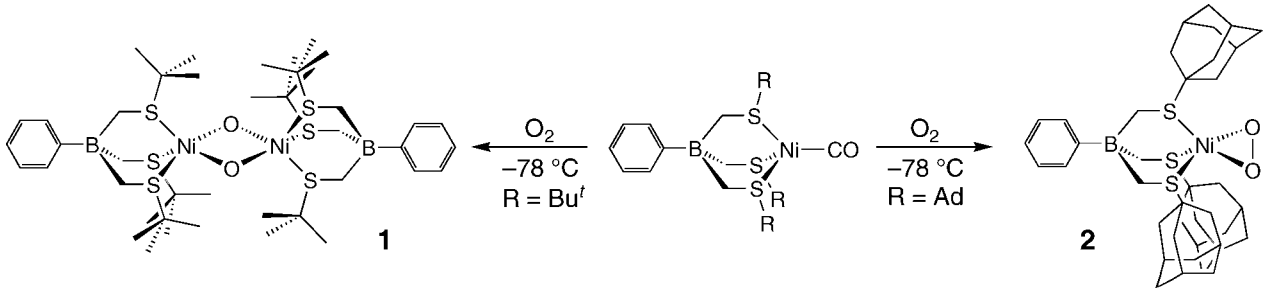

described formation of a bis-μ-superoxo species by exposing $\{[(Me_3\text{-tpa})Ni]_2(\mu\text{-}OH)_2\}^{2+}$ to excess hydrogen peroxide.[27] In related work, Suzuki and co-workers isolated a dinickel $(\mu\text{-}OOR)_2$ complex en route to the ligand C–H activation product.[28] Finally, Walton and co-workers prepared a structurally unique μ^6-peroxo–hexanickel complex.[29]

An attractive alternative entails reaction of a reduced metal precursor with dioxygen, the strategy which we have employed in our work, and for which a notable previous example exists.[30] While investigating the metal-catalyzed oxygenation of isocyanide to isocyanate, Otsuka intercepted a Ni^{2+}–peroxo complex, $Ni(O_2)(^tBuNC)_2$.[30,31] This product is formed via oxidative addition of O_2 to $Ni(^tBuNC)_4$.

A bioinspired strategy aimed at efficient and controlled harnessing of the oxidative power of dioxygen relies in part on the design of molecular systems that make dioxygen more reactive toward substrate hydrocarbons, while avoiding autoxidation and overoxidation. Further, the design of such systems depends on a detailed understanding of the structure–function correlations of metal–dioxygen adducts. Isolation and characterization of unique structure types are of paramount importance. Under this framework, we began our investigations into the activation of dioxygen by nickel complexes. These studies employ monovalent nickel so higher oxidation states of nickel–oxygen adducts can be accessed. The strategy appears limited only by the ability to prepare and isolate stable monovalent precursors. Fortunately, judicious choice of the polydentate ligand affords the requisite starting materials. We describe two such systems in this Account, which led to the interception and characterization of new Ni–O_x structure types.

O_2 Activation Using Tripodal Thioether-Supported Nickel(I)

The tripodal thioether borato ligands developed in these laboratories effectively stabilize transition metal ions in their lower oxidation states.[32,33] Chemical reduction of $[PhTt^R]NiCl$ {$PhTt^R$ = phenyl[tris(alkylthiomethyl)]borate, where R = ^{t}Bu or Ad} by MeLi in the presence of a neutral donor to trap the incipient $[PhTt^R]Ni^+$ fragment affords yellow to orange complexes $[[PhTt^R]Ni(L)$, where L = CO,[33] CN^tBu, PPh_3, or PMe_3]. These thermally stable species are characterized by paramagnetically shifted ^{1}H NMR and EPR spectral signals, the latter detectable only at low temperatures, ca. 10 K. Subambient addition of dry dioxygen to a toluene solution of $[PhTt^{tBu}]Ni(CO)$ leads to a dramatic change in color to deep purple, indicating formation of the bis-μ-oxo dimer, $[(PhTt^{tBu})Ni]_2(\mu\text{-}O)_2$ (**1**) (Scheme 1).[34] The thermally unstable product decays at room temperature with a $t_{1/2}$ of 5 min. **1** displays two intense optical features: λ_{max} (ϵ) = 410 (12000 M^{-1} cm^{-1}) and 565 nm (16000 M^{-1} cm^{-1}). The latter feature is ascribed to a O → Ni CT transition which is ca. 100 nm red-shifted compared to those of similar $Ni_2(\mu\text{-}O)_2$ rhombs supported by nitrogen donor ligands. Resonance Raman spectra of **1** reveal a very intense, isotope sensitive feature at 590 cm^{-1} (560 cm^{-1} in samples of **1** prepared from $^{18}O_2$, consistent with the downshift calculated for a simple harmonic oscillator). The band is assigned as the totally symmetric ν(Ni–O) mode of the $Ni_2(\mu\text{-}O)_2$ core. The excitation profile of the Raman band parallels the 565 nm electronic absorption band, supporting assignment of the latter as a O → Ni CT transition. Furthermore, the frequency of the vibrational band is similar to that of bands found in other $M_2(\mu\text{-}O)_2$ cores (M = Mn, Fe, or Cu). The Ni coordination sphere of **1** is identified by Ni K-edge EXAFS experiments. There are two oxygen scatters at a short distance (1.82 Å) and three sulfurs at 2.34 Å. The Ni ··· Ni vector is clearly discernible at 2.83 Å. The short Ni–O and Ni ··· Ni distances are in agreement with those metrics determined by X-ray diffraction analysis of $[(Tp^{Me3})Ni]_2(\mu\text{-}O)_2$[26] and related $Cu_2(\mu\text{-}O)_2$ cores.[35] Lastly, a low-quality X-ray crystal structure of **1** confirms the molecular con-

Scheme 2

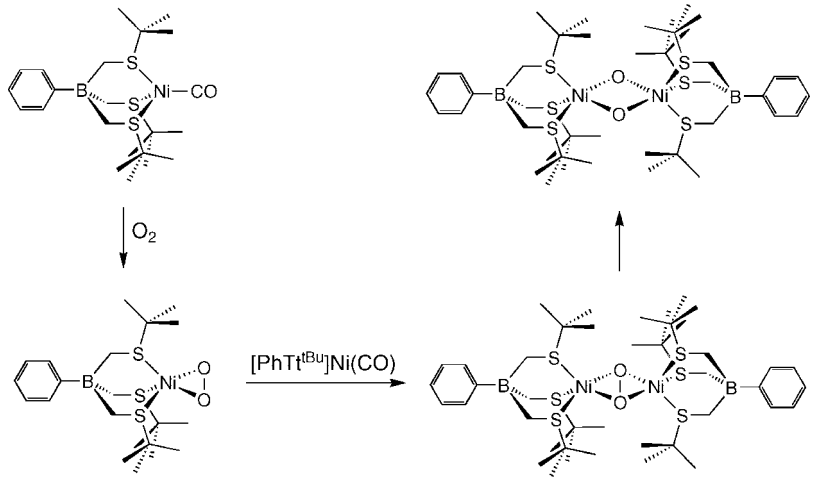

nectivity proposed on the basis of the sum of the spectroscopic characteristics. Unfortunately, the quality of the X-ray data does not permit any quantitative comparisons with either EXAFS- or DFT-derived parameters.

Complex **1** exhibits very limited reactivity with exogenous substrates, presumably due to limited access to the oxidizing core, i.e., a kinetic barrier. At low temperatures, where **1** persists, it does not react with PPh_3, PMe_3, or olefins. **1** oxidizes NO to nitrite, generating [PhTt^{tBu}]Ni(NO_2). The low reactivity of **1** implies that the dimer is not in equilibrium with the monomer, [PhTt^{tBu}]Ni(O), as the latter, albeit unprecedented, structure is anticipated to be highly reactive. There is no evidence of a monomer in solution. Samples of **1** prepared from a mixture of $^{16}O_2$ and $^{18}O_2$ contain only [(PhTt^{tBu})Ni]$_2$(μ-^{16}O)$_2$ and [(PhTt^{tBu})Ni]$_2$(μ-^{18}O)$_2$, as revealed by resonance Raman measurements with no indication of the mixed labeled dimer expected to result from a dimer–monomer equilibrium.

Mononuclear Dioxygen Adduct

We reasoned that ligand modification designed to prevent dimer formation would be a productive approach likely leading to a new type of Ni–O_x complex with a core more accessible to substrate oxidation and providing fundamental insight into the mechanism by which **1** forms from [PhTt^{tBu}]Ni(CO) and O_2. Thus, 1-adamantyl cages were installed as terminal thioether substituents in the tris(thioether)borato framework leading to [PhTt^{Ad}].[36] Satisfyingly, the Ad for ^{t}Bu replacement proved to be straightforward with respect to synthesis of the ligand and desired nickel precursors using the procedures developed for the preparation of [PhTt^{tBu}]Ni(CO). The electronic donor characteristics of the two tripodal ligands are identical as evidenced by the ν(CO) values determined for [PhTt^{tBu}]Ni(CO) (1999 cm^{-1}) and [PhTt^{Ad}]Ni(CO) (1997 cm^{-1}). However, the desired steric impediments to dimer formation are apparent as oxygenation of [PhTt^{Ad}]Ni(CO) proceeds distinctly to a mononuclear adduct, [PhTt^{Ad}]Ni(O_2) (**2**) (Scheme 2).[37]

Like **1**, complex **2** is stable only at low temperatures. The composition and structure of **2** were determined from its unique spectroscopic features, which are distinct from those of **1**, and supported by DFT calculations and its reactivity. The electronic absorption spectrum of **2** contains the following features: λ_{max} (ϵ) = 310 (5900 M^{-1} cm^{-1}), 386 (2900 M^{-1} cm^{-1}), 450 (2500 M^{-1} cm^{-1}), and 845 nm (350 M^{-1} cm^{-1}). Unfortunately, resonance Raman spectral experiments were unsuccessful in identifying any oxygen isotope sensitive vibrational features in **2**, perhaps due to a weak $[NiO_2]^+$ absorption chromophore.

The magnetic characteristics of **2** include paramagnetically shifted ^{1}H NMR spectral resonances and an $S = {}^1/_2$ EPR signal at 4 K. The rhombic EPR signal with effective g values of 2.24, 2.19, and 2.01 is in accord with the unpaired electron residing in the d_{z^2} orbital, an assignment supported by DFT calculations. The coordination sphere in **2** has been defined by Ni EXAFS measurements; crystals suitable for single-crystal X-ray diffraction have yet to be isolated. The three Ni–S distances average to 2.26 Å, and the two Ni–O distances are 1.85 Å. While the assignment of coordination number by EXAFS precludes unequivocal establishment of end-on versus side-on O_2 ligation, the data are fit much better assuming the latter motif. The mode of O_2 ligation in **2** is supported further by computational analysis of hypothetical end-on and side-on [PhTt^{Ad}]Ni(O_2) species. Semiempirical INDO/S-CI computations on DFT-minimized structures yielded principal g values for the side-on O_2 complex (g = 2.29, 2.22, and 2.09) that are in much better agreement with the experimentally determined effective g values. Furthermore, the DFT computations determined the side-on complex to be energetically favored by ~10 kcal/mol compared to an end-on complex. Thus, the assignment of **2** as a side-on dioxygen complex is supported by its lower energy relative to the end-on isomer and the fact that parameters derived from calculations of the side-on structure are in better agreement with the observables from two independent experimental measurements, i.e., Ni EXAFS and EPR data.[37]

Next, we turn our attention to understanding the electronic structure of **2**. The ν(O–O) vibrational energy provides insight into the extent of charge transfer ac-

companying O_2 ligation.[38] However, as mentioned previously, resonance Raman experiments failed to detect this mode. Therefore, DFT computations were used to provide insight. The computed O–O distance of 1.38 Å implies superoxo character as calculations on peroxo complexes generally yield O–O distances longer than 1.4 Å. The Ni XAS displays a pre-edge 1s → 3d transition at 8331.4 eV. The value is intermediate between that of the Ni^+ precursors and the Ni^{3+} dimer, **1**, and is, therefore, consistent with a Ni^{2+} description. Relevant natural orbitals reveal the HOMO to be the predominant σ-bonding orbital, showing nearly equal contributions from Ni $d_{x^2-y^2}$ and O_2 π^* orbitals. Inspection of the SOMO, largely Ni d_{z^2}, provides a rationale for the EPR spectral features and the lack of discernible hyperfine broadening of the signal of [PhTt^{Ad}]Ni($^{17}O_2$). Conversely, ^{61}Ni ($I = {}^3/_2$)-enriched samples of **2** show significant hyperfine coupling in g_3, A_3 (^{61}Ni) = 31 G. While we described the geometric and electronic structure parameters as being consistent with a Ni^{2+}–superoxo formalism, others have suggested greater charge transfer on the basis of the computed O–O bond length and, thus, a molecule further along the continuum toward a Ni^{3+}–peroxo complex.[39]

As anticipated, the reactivity of **2** is more extensive than that displayed by **1**, likely because the oxidizing core in the former is more accessible. Additionally, the inherent thermodynamic preferences for oxidation should be distinct between the two structures. In a stoichiometric reaction, **2** oxidizes PPh_3 to $OPPh_3$ with incorporation of the ^{18}O label into $OPPh_3$ confirming O_2 as the source. **2** transforms NO to nitrate in forming [PhTt^{Ad}]Ni(NO_3). Lastly, **2** oxidizes [PhTt^{tBu}]Ni(CO) to the nonsymmetric dimer, [PhTt^{Ad}]Ni(μ-O)$_2$Ni[PhTt^{tBu}]. The latter reaction highlights the synthetic utility of **2** for the preparation of nonsymmetric and mixed metal complexes. In a conceptually related example, a heterobinuclear NiCu(μ-O)$_2$ species was prepared by the condensation of the Cu^{3+}–peroxo complex, [((Pr^i)$_2$$C_6H_3$NC($CH_3$))$_2$CH]Cu($O_2$), with the [PhTt^{tBu}]Ni(CO) precursor.[40]

Interception and characterization of **2** upon oxygenation of the Ni^+ precursor implicate an analogous species, [PhTt^{tBu}]Ni(O_2), as an intermediate on the pathway to formation of **1**. Thus, with a complete understanding of the spectral characteristics of **2** in hand, we revisited the oxygenation reaction leading to **1**. Indeed, the reaction proceeds via an intermediate with optical and EPR spectral characteristics similar to those observed for **2**. [PhTt^{tBu}]-Ni(O_2) decays yielding **1**, thus indicating that [PhTt^{tBu}]-Ni(O_2) is an intermediate on the pathway to bis-μ-oxo dimer formation.

Next, we address the process of dimerization leading to **1**, specifically the issue of whether a μ-η^2:η^2-peroxo intermediate was along the reaction trajectory (Scheme 2). This canonical mechanism is inspired by the well-established dioxygenation pathway for Cu^+ and is used as a framework for considering similar Ni^+-based reactions. While the μ-η^2:η^2-peroxo structure type remains unprecedented for nickel, there are a number of examples of dicopper complexes beginning with the landmark

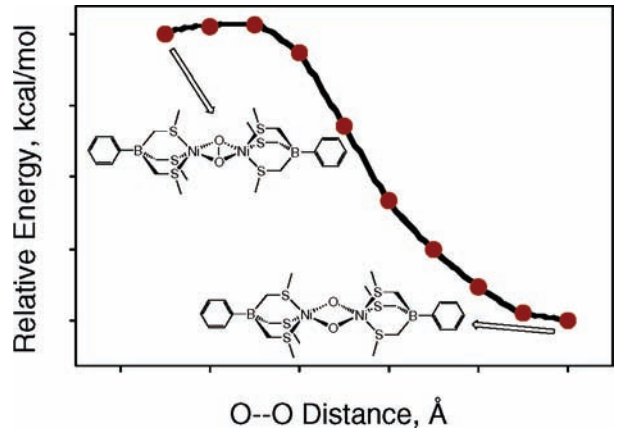

FIGURE 2. Relative total energies of molecules derived from DFT point calculations along a hypothetical reaction trajectory from μ-η^2:η^2-peroxo– to bis-μ-oxo–dinickel cores. Each point reflects the total energy at a fixed O–O distance.

studies of Kitajima.[41] Of further interest is the observation that for certain Cu complexes the μ-η^2:η^2-peroxo and bis-μ-oxo isomers are in equilibrium and, therefore, necessarily similar in energy.[42] Lacking experimental evidence in support of a μ-η^2:η^2-peroxo–dinickel complex, we explored the conversion from μ-η^2:η^2-peroxo to the bis-μ-oxo isomer via a series of DFT computations.[43] The molecular structure and energy of putative [(PhTt)Ni]$_2$(μ-η^2:η^2-O_2) (with methyl thioether substituents) were determined using a symmetry-unrestricted DFT geometry optimization. The final structure contained an O–O bond length consistent with a bridging peroxide ligand (1.489 Å). Additional structures along a hypothetical reaction pathway were generated by increasing the O–O distance incrementally, with other degrees of freedom fully relaxed. The results, summarized in Figure 2, reveal a significant stabilization of **1** by 32 kcal/mol with a minimum activation barrier (2.0 kcal/mol) for the conversion. Thus, compared to copper, the Ni$_2$(μ-O)$_2$ core is greatly stabilized relative to its Ni$_2$(μ-η^2:η^2-O_2) isomer. The difference between the Cu and Ni cases may be appreciated by examining the degree of M d_{xy} → $(O_2)^{2-}$ σ_u* donation in the M$_2$(μ-η^2:η^2-O_2) structures. More effective back donation weakens the O–O bond, with the limit amounting to rupture of this bond, i.e., formation of the bis-μ-oxo isomer. The lower effective nuclear charge of Ni^{2+} (Z_{eff} = 7.2) relative to that of Cu^{2+} (Z_{eff} = 7.85) means the Ni d-orbitals are much higher in energy. This results in a smaller energy gap with the peroxo σ_u* and more effective back donation.

While this rationale emphasizes the importance of electronic effects in governing formation of the bis-μ-oxo–dinickel complex, steric control plays a predominant role in directing the course of structure formation in metal–dioxygen chemistry. Thus, in this case, introduction of the appropriately sized ligand substituents may provide an opportunity to access a Ni$_2$(μ-η^2:η^2-O_2) core. Using the [PhTt^R] ligand class, this challenge is significant as the desired substituent should be larger than *tert*-butyl, as [PhTt^{tBu}] leads to **1**, yet smaller than 1-adamantyl, which leads to monomeric **2**.

Scheme 3

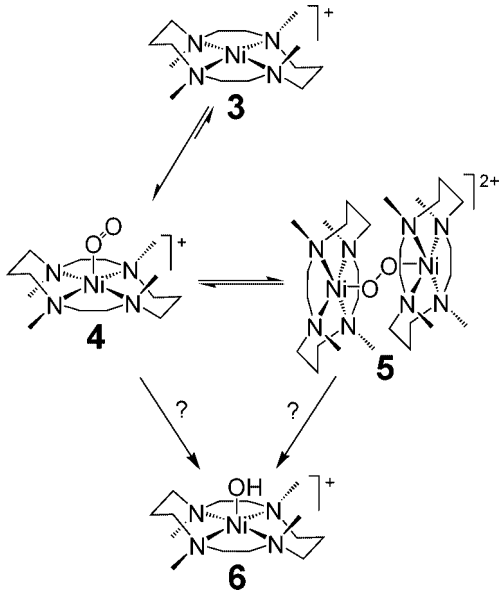

O_2 Activation Using a Ni(I)–Tetraazamacrocycle Complex

To access a peroxo species via the strategy of dioxygen activation by monovalent nickel, we hypothesized that elimination of vacant cis coordination sites on the metal would enforce "end-on" dioxygen coordination and preclude over-reduction to the thermodynamically favorable bis-μ-oxo–dinickel core. To meet this demand, we employed a ligand shown previously to be capable of supporting nickel(I), tmc [1,4,8,11-tetramethyl-1,4,8,11-tetraazacyclotetradecane (Scheme 3)].[44] Prior efforts from this laboratory focused on oxidation of [Ni(tmc)]OTf (OTf = $CF_3SO_3^-$) by thiols, disulfides, and organocobalt reagents.[45,46] [Ni(tmc)]OTf is prepared by chemical reduction of [Ni(tmc)]$(OTf)_2$, typically with sodium mercury amalgam. Unless specified, the following studies were performed using the *RRSS* isomer exclusively.

Addition of excess dioxygen to a solution of [Ni(tmc)](OTf) (**3**) results in formation of a green solution over the course of hours. On the basis of IR, ^{1}H NMR, and ESI MS analyses, the product was determined to be [Ni(tmc)(OH)]OTf (**6**).[47] Independent preparation of **6** via the metathesis of [Ni(tmc)]$(OTf)_2$ with KOH supports the assignment. Oxygenation of **3** in d_3-acetonitrile yielded [Ni(tmc)(OD)]OTf, whereas oxygenation with $^{18}O_2$ resulted in incorporation of ^{18}O into the product. In sum, these experiments indicate the source of the oxygen in the hydroxo ligand is dioxygen and the hydrogen is derived from acetonitrile solvent.

Addition of excess dioxygen to **3** at low temperatures and tracking of the reaction progress optically reveal the formation of two transient intermediates. The first observed intermediate is the peroxo-bridged dimer **5** (Scheme 3).[47] The deep red color of **5** [λ_{max} (ε) = 465 nm (2100 M^{-1} cm^{-1}/Ni)] forms nearly instantaneously upon oxygenation. The lifetime of **5** ($t_{1/2}$ = 5 min at −60 °C) is long enough to permit its spectroscopic evaluation. The most important data to support the assignment as a μ-1,2-peroxo–dinickel complex are the resonance Raman and magnetic (NMR and EPR) spectral characteristics. Optical excitation of samples of **5** near the dominant absorption feature (λ_{ex} = 503 nm) reveals two oxygen isotope-sensitive features. The intraperoxide stretch is found at 778 cm^{-1} (735 cm^{-1} in samples prepared from $^{18}O_2$). The energy and magnitude of isotope sensitivity are within the range of values expected for a peroxo ligand. The ν(Ni–O) band appears at a much lower intensity and frequency [479 cm^{-1} ($^{18}O_2$-derived sample, 456 cm^{-1})]. Complex **5** is EPR silent while exhibiting a paramagnetic ^{1}H NMR spectrum, indicative of an integer spin state, e.g., a dimer. Density functional theory provides insight in support of this conclusion, vide infra.[48] The energy of the Raman band is somewhat low compared to those of trans-μ-1,2 peroxo complexes of Co[49] and Cu.[50]

Interestingly, DFT predicts an anti-ferromagnetically coupled diamagnetic $M_S = 0$ ground state for **5**, in contrast to the observed paramagnetism. Evaluation of the NMR spectral characteristics by measurement of the temperature dependence of **5** reveals non-Curie chemical shift behavior, a hallmark of a species with a low-lying, and thermally accessible paramagnetic excited state.[51] DFT affirms this notion, predicting a low J value of ~220 cm^{-1}, and consequently a relatively inefficient superexchange pathway when compared to Cu systems ($J \sim 600$ cm^{-1}).[52] In summary, **5** is the trans-μ-1,2-peroxo–nickel dimer with a diamagnetic $S = 0$ ground state.

The second intermediate observed optically is **4**, a green-brown mononuclear nickel–superoxo adduct.[53] This species has a much longer lifetime then **5**, exhibiting a half-life of hours at room temperature. Resonance Raman excitation into the dominant absorption envelope (λ_{ex} = 364 nm) enhances an oxygen isotope sensitive feature at 1131 cm^{-1}. The energy and isotope sensitivity (1065 cm^{-1} in samples prepared with $^{18}O_2$) of this feature are consistent with assignment as a superoxo, ν(O–O) mode. Complex **4** is EPR active, displaying a rhombic signal with g values of 2.29, 2.21, and 2.09, in accord with an $S = {}^1/_2$ ground state. The Ni K-edge X-ray absorption spectrum of **4** contains a weak 1s → 3d pre-edge feature at 8333.9 eV, providing support for the Ni^{2+} formulation.

It was initially surprising that the 1:1 adduct **4** was forming *after* observation of the corresponding dimer, **5**. The most straightforward interpretation is that addition of dioxygen to both **3** and **5** is rate-limiting, indicating that $[Ni(tmc)]^+$ reacts with $[Ni(tmc)O_2]^+$ faster than it reacts with dioxygen. This interpretation is substantiated by the fact that attempts to observe the formation of **4** en route to **5** by cryogenic stopped-flow experiments have proven to be unsuccessful. Complex **5** forms upon addition of dioxygen to **3** with isosbestic behavior. Low-temperature addition of **3** to solutions of **4** and vice versa result in rapid formation of **5**. Lastly, subjecting **4** to an extended Ar purge at low temperatures does not promote O_2 loss, which suggests a substantially stabilized dioxygen adduct. Collectively, these observations suggest that the formation of **5** is under kinetic control and binding of O_2 is rate-limiting.

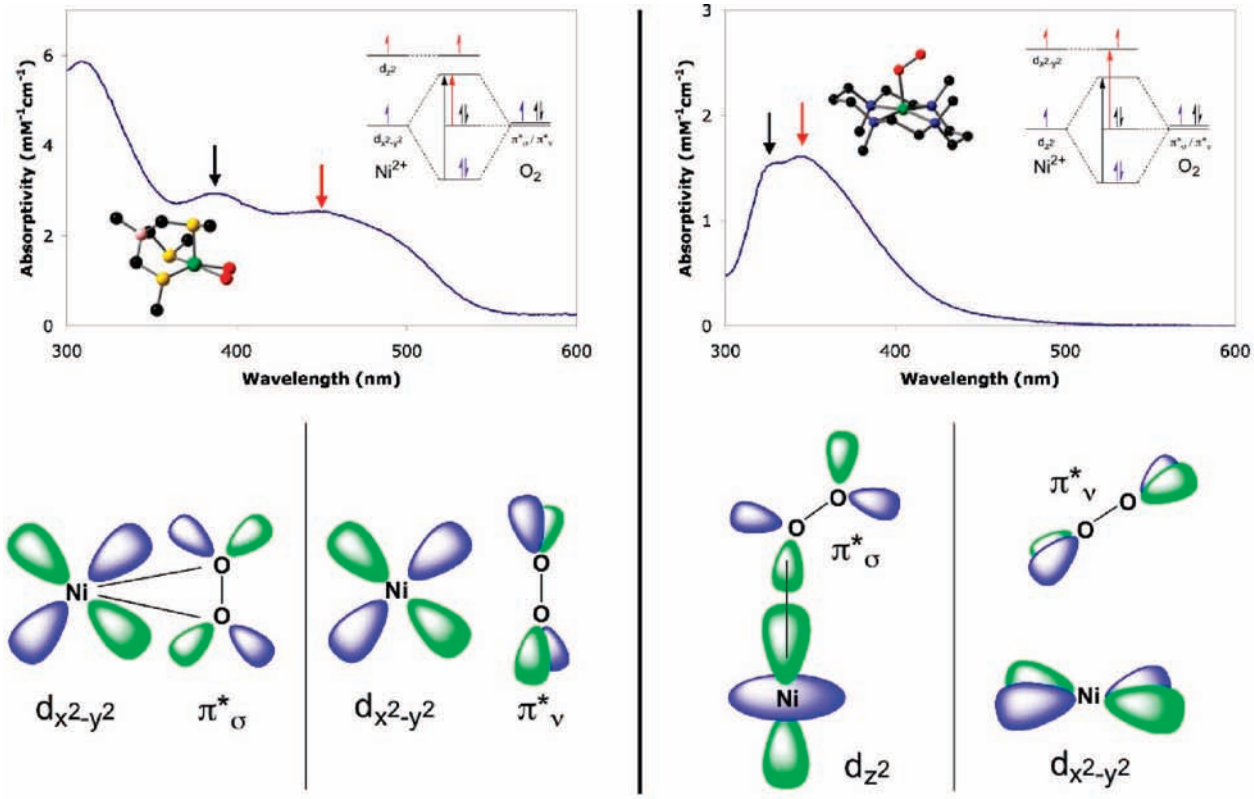

FIGURE 3. Optical spectrum of **2** with LMCT transitions denoted by arrows (left). The inset shows a qualitative MO diagram. Bonding description derived from natural orbitals (bottom left). Optical spectrum of **4** with LMCT transitions denoted by arrows (right). The inset shows a qualitative MO diagram. Bonding description derived from natural orbitals (bottom right).

Comparison of "Side-On" and "End-On" Ni^{2+}–Superoxo Complexes

Despite differences in O_2 coordination geometry in their molecular structures, **2** and **4** share similar electronic structures. Both species can be formally described as Ni^{2+}–superoxo complexes. A low-spin (LS) $M_S = {}^1/_2$ configuration is observed by EPR spectroscopy in both cases, with the majority of unpaired spin density localized on the nickel, not on the dioxygen. This scenario is not unexpected, as illustrated qualitatively by the key bonding interactions (Figure 3), derived from DFT computations.

In the case of **2**, the interaction is dominated by in-plane overlap of the singly occupied Ni $d_{x^2-y^2}$ orbital with the singly occupied O_2 π^* orbital leading to coupling of these electrons. The nickel d_{z^2} orbital is strongly destabilized in the square pyramidal geometry, and consequently, it is the singly occupied molecular orbital (SOMO). The orbital description accounts for the EPR signal, particularly the observed ^{61}Ni hyperfine splitting and lack of discernible $^{17}O_2$ coupling. Two ligand-to-metal charge transfer (LMCT) O_2-related absorption features are expected and observed. However, the most dominant feature in the spectrum is the result of the thioether LMCT at high (305 nm) energy.

The electronic description of **4** is akin to that of **2**. In this case, the coordinate system is defined differently with the dioxygen ligand residing along the z vector. The Ni $d_{x^2-y^2}$ orbital is the SOMO due to strong interaction with the amines of the macrocycle. Interestingly, and due to the sterics imposed by tmc, overlap of the O_2 π^* orbital pair with the symmetry appropriate Ni orbitals results in weaker transitions at higher energy. Direct comparison of the observed g-tensors in both **2** and **4** is uninformative because of the differences in coordination geometry and supporting ligand. Further, due to the fact that resonance Raman data are not yet available for **2**, assessing the level of reduction of O_2 is confined to the results of DFT analysis, notably the O–O bond lengths. In this context, **2** possesses a significantly more reduced dioxygen moiety compared to **4**. Experiments in which a more direct probe of the extent to which O_2 is reduced for further comparison of these structure types are underway, most notably ligand modification to aid in nucleation of single crystals.

Future Directions

Research objectives emphasized in this Account have included establishing the geometric and electronic structures of new complexes derived from the reaction of nickel(I) precursors with dioxygen. The strategy represents a compelling and different approach to preparing such metastable, reactive intermediates inspired by the rich biomimetic studies of copper complexes. These investigations have only touched upon exogenous substrate oxidations, reasoning that a thorough understanding of the complexes' structures and spectroscopic characteristics are requisite. Nonetheless, a number of earlier studies utilizing nickel(II) and oxygen atom transfer reagents, e.g., iodosylbenzene, demonstrated that the resulting oxidant

is potent for a range of intermolecular transformations utilizing a diverse substrate scope.[54–56] Efforts to establish the compositions of these intermediates will provide a deeper understanding of the structure–function correlations that define contemporary chemistry and perhaps yield insight into the rationale governing the absence of nickel-based aerobic enzyme oxidants. The development of nickel reagents for stoichiometric and catalytic oxidations represents an attractive area of endeavor, in part given the utility of its heavy metal congener, palladium,[57] in oxidation catalysis. The significantly lower cost of nickel makes this objective economically alluring.

Summary

The activation of dioxygen by monovalent nickel complexes has provided access to a range of new geometric and electronic structure types as deduced by in situ spectroscopic examination of thermally sensitive intermediates, supported by complementary reactivity studies and density functional theory calculations. On the basis of the results obtained for the two different systems described herein, several general observations are warranted. Ligand design is significant in both stabilizing the lower-valent oxidation state and directing the course of the reactions with O_2. Precursors with available cis coordination sites favor side-on O_2 ligation and access to O–O bond rupture via formation of bis-μ-oxo–dinickel species. Theoretical analysis of a putative μ-η^2:η^2-peroxo–dinickel complex established the species to be significantly destabilized relative to its bis-μ-oxo isomer and provided a rationale for differences in the relative energetics of the dicopper and dinickel adducts. Complexes possessing a planar tetradentate ligand lead to end-on peroxo dinickel and superoxo species. The side-on and end-on Ni^{2+}–superoxo adducts have similar electronic structures, with the former containing a somewhat more reduced O_2 ligand, and promote the transfer of an oxygen atom to PPh_3.

The National Science Foundation has supported these nickel–dioxygen studies. Some of the calculations described have been performed at the INBRE Bioinformatics Center of the University of Arkansas for the Medical Sciences (NIH Grant P20 RR-16460). We are indebted to the talented co-workers in the laboratory critical to the development of the chemistry described herein, Peter J. Schebler, Beaven S. Mandimutsira, Koyu Fujita, and Sharon R. Hatalla. Enjoyable and productive collaborations with Professors Thomas C. Brunold and Stephen P. Cramer and their co-workers, Ralph Schenker, Katherine M. Van Heuvelen, and Weiwei Gu, have greatly advanced our understanding of the structures of unstable intermediates. Collaborations with Professors Bill Tolman and Wonwoo Nam further enriched these studies.

References

(1) Meunier, B., Ed. *Biomimetic Oxidations Catalyzed by Transition Metal Complexes*; Imperial College Press: London, 2000.
(2) Hlavica, P. Models and mechanisms of O-O bond activation by cytochrome P450: A critical assessment of the potential role of multiple active intermediates in oxidative catalysis. *Eur. J. Biochem.* **2004**, *271*, 4335–4360.
(3) Decker, A.; Solomon, E. I. Dioxygen activation by copper, heme and non-heme iron enzymes: Comparison of electronic structures and reactivities. *Curr. Opin. Chem. Biol.* **2005**, *9*, 152–163.
(4) Ragsdale, S. W. Life with Carbon Monoxide. *Crit. Rev. Biochem. Mol. Biol.* **2004**, *39*, 165–195.
(5) Lindahl, P. A. Acetyl-coenzyme A synthase: The case for a $Ni_p(0)$-based mechanism of catalysis. *J. Biol. Inorg. Chem.* **2004**, *9*, 516–524.
(6) Dobbek, H.; Svetlitchnyi, V.; Gremer, L.; Huber, R.; Meyer, O. Crystal Structure of a Carbon Monoxide Dehydrogenase Reveals a [Ni-4Fe-5S] Cluster. *Science* **2001**, *293*, 1281–1285.
(7) Shima, S.; Thauer, R. K. Methyl-coenzyme M reductase and the aerobic oxidation of methane in methanotropic Archea. *Curr. Opin. Microbiol.* **2005**, *8*, 643–648.
(8) Leclere, V.; Boiron, P.; Blondeau, R. Diversity of Superoxide-Dismutases Among Clinical and Soil Isolates of *Streptomyces* Species. *Curr. Microbiol.* **1999**, *39*, 365–368.
(9) Youn, H.-D.; Kim, E.-J.; Roe, J.-H.; Hah, Y. C.; Kang, S.-O. A novel nickel-containing superoxide dismutase from *Streptomyces* spp. *Biochem. J.* **1996**, *318*, 889–896.
(10) Youn, H.-D.; Youn, H.; Lee, J.-W.; Yim, Y.-I.; Lee, J. K.; Hah, Y. C.; Kang, S.-O. Unique Isozymes of Superoxide Dismutase in *Streptomyces griseus*. *Arch. Biochem. Biophys.* **1996**, *334*, 341–348.
(11) Palenik, B.; Brahamsha, B.; Larimer, F. W.; Land, M.; Hauser, L.; Chain, P.; Lamerdin, J.; Regala, W.; Allen, E. E.; McCarren, J.; Paulsen, I.; Dufresne, A.; Partensky, F.; Webb, E. A.; Waterbury, J. The genome of a motile marine *Synechococcus*. *Nature* **2003**, *424*, 1037–1042.
(12) Wuerges, J.; Lee, J.-W.; Yim, Y.-I.; Yim, H.-S.; Kang, S.-O.; Carugo, K. D. Crystal structure of nickel-containing superoxide dismutase reveals another type of active site. *Proc. Natl. Acad. Sci. U.S.A.* **2004**, *125*, 8569–8574.
(13) Choudhury, S. B.; Lee, J.-W.; Davidson, G.; Yim, Y.-I.; Bose, K.; Sharma, M. L.; Kang, S.-O.; Cabelli, D. E.; Maroney, M. J. Examination of the Nickel Site Structure and Reaction Mechanism in *Streptomyces seoulensis* Superoxide Dismutase. *Biochemistry* **1999**, *38*, 3744–3752.
(14) Fiedler, A. T.; Bryngelson, P. A.; Maroney, M. J.; Brunold, T. C. Spectroscopic and Computational Studies of Ni Superoxide Dismutase: Electronic Structure Contributions to Enzymatic Function. *J. Am. Chem. Soc.* **2005**, *127*, 5449–5462.
(15) Pelmenschikov, V.; Siegbahn, P. E. M. Nickel Superoxide Dismutase Reaction Mechanism Studied by Hybrid Density Functional Methods. *J. Am. Chem. Soc.* **2006**, *128*, 7466–7475.
(16) Dai, Y.; Wensink, P. C.; Abeles, R. H. One Protein, Two Enzymes. *J. Biol. Chem.* **1999**, *274*, 1193–1195.
(17) Dai, Y.; Pochapsky, T. C.; Abeles, R. H. Mechanistic Studies of Two Dioxygenases in the Methionine Salvage Pathway of *Klebsiella pneumoniae*. *Biochemistry* **2001**, *40*, 6379–6387.
(18) Al-Mjeni, F.; Ju, T.; Pochapsky, T. C.; Maroney, M. J. XAS Investigation of the Structure and Function of Ni in Acireductone Dioxygenase. *Biochemistry* **2002**, *41*, 6761–6769.
(19) Szajna, E.; Arif, A. M.; Berreau, L. M. Aliphatic Carbon-Carbon Bond Cleavage Reactivity of a Mononuclear Ni(II) cis-β-Keto-Enolate Complex in the Presence of Base and O_2: A Model Reaction for Acireductone Dioxygenase (ARD). *J. Am. Chem. Soc.* **2005**, *127*, 17186–17187.
(20) Bal, W.; Djuran, M. I.; Margerum, D. W.; Edward, T.; Gray, J.; Mazid, M. A.; Tom, R. T.; Nieboer, E.; Sadler, P. J. Dioxygen-induced Decarboxylation and Hydroxylation of [Ni^{II}(Glycyl-Glycyl-L-Histidine)] Occurs via Ni^{III}: X-Ray Crystal Structure of [Ni^{II}(Glycyl-Glycyl-α-hydroxy-D,L-Histamine)]·$3H_2O$. *J. Chem. Soc., Chem. Commun.* **1994**, 1889–1890.
(21) Grapperhaus, C. A.; Darensbourg, M. Y. Oxygen Capture by Sulfur in Nickel Thiolates. *Acc. Chem. Res.* **1998**, *31*, 451–459.
(22) Kimura, E.; Machida, R.; Kodama, M. Macrocyclic Dioxo Pentaamines: Novel Ligands for 1:1 Ni(II)-O_2 Adduct Formation. *J. Am. Chem. Soc.* **1984**, *106*, 5497–5505.
(23) Kimura, E.; Machida, R. A Mono-oxygenase Model for Selective Aromatic Hydroxylation with Nickel(II)-Macrocyclic Polyamines. *J. Chem. Soc., Chem. Commun.* **1984**, 499–500.
(24) Chen, D.; Martell, A. E. Oxygen Insertion in the Ni(II) Complexes of Dioxopentaaza Macrocyclic Ligands. *J. Am. Chem. Soc.* **1990**, *112*, 9411–9412.
(25) Cheng, C.-C.; Gulia, J.; Rokita, S. E.; Burrows, C. J. Dioxygen chemistry of nickel(II) dioxopentaazamacrocyclic complexes: Substituent and medium effects. *J. Mol. Catal. A: Chem.* **1996**, *113*, 379–391.
(26) Hikichi, S.; Yoshizawa, M.; Sasakura, Y.; Akita, M.; Moro-oka, Y. First Synthesis and Structural Characterization of Dinuclear M(III) Bis(μ-oxo) Complexes of Nickel and Cobalt with Hydrotris(pyrazolyl)borate Ligand. *J. Am. Chem. Soc.* **1998**, *120*, 10567–10568.

(27) Shiren, K.; Ogo, S.; Fujinami, S.; Hayashi, H.; Suzuki, M.; Uehara, A.; Watanabe, Y.; Moro-oka, Y. Synthesis, Structures, and Properties of Bis(μ-oxo)nickel(III) and Bis(μ-superoxo)nickel(II) Complexes: An Unusual Conversion of a $Ni^{III}_2(\mu\text{-}O)_2$ Core into a $Ni^{II}_2(\mu\text{-}OO)_2$ Core by H_2O_2 and Oxygenation of Ligand. *J. Am. Chem. Soc.* **2000**, *122*, 254–262.

(28) Cho, J.; Furutachi, H.; Fujinami, S.; Suzuki, M. A Bis(μ-alkylperoxo)dinickel(II) Complex as a Reaction Intermediate for the Oxidation of the Methyl Groups of the Me_2-tpa Ligand to Carboxylate and Alkoxide Ligands. *Angew. Chem., Int. Ed.* **2004**, *43*, 3300–3303.

(29) Brown, E. J.; Duhme-Klair, A.-K.; Elliott, M. I.; Thomas-Oates, J. E.; Timmins, P. L.; Walton, P. H. The First μ^6-Peroxide Transition-Metal Complex: $[Ni_8(L)_{12}(O_2)]^{2+}$. *Angew. Chem., Int. Ed.* **2005**, *44*, 1392–1395.

(30) Otsuka, S.; Nakamura, A.; Tatsuno, Y. Oxygen Complexes of Nickel and Palladium. Formation, Structure, and Reactivities. *J. Am. Chem. Soc.* **1969**, *91*, 6994–6999.

(31) Matsumoto, M.; Nakatsu, K. Dioxygen-bis-(t-butylisocyanide)nickel. *Acta. Crystallogr.* **1975**, *B31*, 2711–2713.

(32) DuPont, J. A.; Coxey, M. B.; Schebler, P. J.; Incarvito, C. D.; Dougherty, W. G.; Yap, G. P. A.; Rheingold, A. L.; Riordan, C. G. High-Spin Organocobalt(II) Complexes in a Thioether Coordination Environment. *Organometallics* **2007**, *26*, 971–979.

(33) Schebler, P. J.; Mandimutsira, B. S.; Riordan, C. G.; Liable-Sands, L. M.; Incarvito, C. D.; Rheingold, A. L. Organometallic Cobalt(II) and Nickel(II) Complexes Supported by Thioether Ligation: Unexpected Nickel Alkylation by the Borato Ligand Phenyltris((tert-butylthio)methyl)borate. *J. Am. Chem. Soc.* **2001**, *123*, 331–332.

(34) Mandimutsira, B. S.; Yamarik, J. L.; Brunold, T. C.; Gu, W.; Cramer, S. P.; Riordan, C. G. Dioxygen Activation by a Nickel Thioether Complex: Characterization of a $Ni^{III}_2(\mu\text{-}O)_2$ Core. *J. Am. Chem. Soc.* **2001**, *123*, 9194–9195.

(35) Mirica, L. M.; Ottenwaelder, X.; Stack, T. D. P. Structure and Spectroscopy of Copper-Dioxygen Complexes. *Chem. Rev.* **2004**, *104*, 1013–1045.

(36) Fujita, K.; Rheingold, A. L.; Riordan, C. G. Thioether-ligated nickel(I) complexes for the activation of dioxygen. *Dalton Trans.* **2003**, 2004–2008.

(37) Fujita, K.; Schenker, R.; Gu, W.; Brunold, T. C.; Cramer, S. P.; Riordan, C. G. A Monomeric Nickel-Dioxygen Adduct Derived from a Nickel(I) Complex and O_2. *Inorg. Chem.* **2004**, *43*, 3324–3326.

(38) Cramer, C. J.; Tolman, W. B.; Theopold, K. H.; Rheingold, A. L. Variable character of O-O and M-O bonding in side-on (η^2) 1:1 metal complexes of O_2. *Proc. Natl. Acad. Sci. U.S.A.* **2003**, *100*, 3635–3640.

(39) Aboelella, N. W.; Kryatov, S. V.; Gherman, B. F.; Brennessel, W. W.; Victor, G.; Young, J.; Sarangi, R.; Rybak-Akimova, E. V.; Hodgson, K. O.; Hedman, B.; Solomon, E. I.; Cramer, C. J.; Tolman, W. B. Dioxygen Activation at a Single Copper Site: Structure, Bonding, and Mechanism of Formation of 1:1 Cu-O Adducts. *J. Am. Chem. Soc.* **2004**, *126*, 16896–16911.

(40) Aboelella, N. W.; York, J. T.; Reynolds, A. M.; Fujita, K.; Kinsinger, C. R.; Cramer, C. J.; Riordan, C. G.; Tolman, W. B. Mixed metal bis(μ-oxo) complexes with $[CuM(\mu\text{-}O)_2]^{n+}$ (M = Ni(III) or Pd(II)) cores. *Chem. Commun.* **2004**, 1716–1717.

(41) Kitajima, N.; Fujisawa, K.; Moro-oka, Y. μ-η^2:η^2-Peroxo Binuclear Copper Complex, $[Cu(HB(3,5\text{-}iPr_2Pz)_3)]_2(O_2)$. *J. Am. Chem. Soc.* **1989**, *111*, 8975–8976.

(42) Tolman, W. B. Making and Breaking the Dioxygen O-O Bond: New Insights from Studies of Synthetic Copper Complexes. *Acc. Chem. Res.* **1997**, *30*, 227–237.

(43) Schenker, R.; Mandimutsira, B. S.; Riordan, C. G.; Brunold, T. C. Spectroscopic and Computational Studies on $[(PhTt^{tBu})_2Ni_2(\mu\text{-}O)_2]$: Nature of the Bis-$\mu$-oxo $(Ni^{3+})_2$ "Diamond" Core. *J. Am. Chem. Soc.* **2002**, *124*, 13842–13855.

(44) Barefield, E. K.; Freeman, G. M.; Derveer, D. G. V. Electrochemical and Structural Studies of Nickel(II) Complexes of N-Alkylated Cyclam Ligands: X-ray Structures of trans-$[Ni(C_{14}H_{32}N_4)(OH_2)_2]$-$Cl_2\cdot 2H_2O$ and $[Ni(C_{14}H_{32}N_4)](O_3SCF_3)_2$. *Inorg. Chem.* **1986**, *25*, 552–558.

(45) Ram, M. S.; Riordan, C. G.; Ostrander, R.; Rheingold, A. L. Syntheses, Reactivity, and Molecular Structures of RSRS-$[Ni(tmc)SC_6H_5](PF_6)$, RRSS-$[Ni(tmc)SC_6H_5](CF_3SO_3)$, and RRSS-$[Ni(tmc)](CF_3SO_3)$ (tmc = 1,4,8,11-tetramethyl-1,4,8,11-tetraazacyclotetradecane). *Inorg. Chem.* **1995**, *34*, 5884–5892.

(46) Ram, M. S.; Riordan, C. G.; Yap, G. P. A.; Liable-Sands, L.; Rheingold, A. L.; Marchaj, A.; Norton, J. R. Kinetics and Mechanism of Alkyl Transfer from Organocobalt(III) to Nickel(I): Implications for the Synthesis of Acetyl Coenzyme A by CO Dehydrogenase. *J. Am. Chem. Soc.* **1997**, *119*, 1648–1655.

(47) Kieber-Emmons, M. T.; Schenker, R.; Yap, G. P. A.; Brunold, T. C.; Riordan, C. G. Spectroscopic Elucidation of a Peroxo $Ni_2(\mu\text{-}O_2)$ Intermediate Derived from a Nickel(I) Complex and Dioxygen. *Angew. Chem., Int. Ed.* **2004**, *43*, 6716–6718.

(48) Schenker, R.; Kieber-Emmons, M. T.; Riordan, C. G.; Brunold, T. C. Spectroscopic and Computational Studies on the Trans-μ-1,2-Peroxo-Bridged Dinickel(II) Species $[\{Ni(tmc)\}_2(O_2)](OTf)_2$: Nature of End-On Peroxo-Nickel(II) Bonding and Comparison with Peroxo-Copper(II) Bonding. *Inorg. Chem.* **2005**, *44*, 1752–1762.

(49) Barraclough, C. G.; Lawrance, G. A. Evidence for a New μ-Peroxo Binuclear Cobalt(III) Complex of a Macrocyclic Tetraamine from Raman Spectroscopy. *Inorg. Nucl. Chem. Lett.* **1976**, *12*, 133–136.

(50) Jacobson, R. R.; Tyeklar, Z.; Farooq, A.; Karlin, K. D.; Liu, S.; Zubieta, J. A Cu_2-O_2 Complex. Crystal Structure and Characterization of a Reversible Dioxygen Binding System. *J. Am. Chem. Soc.* **1988**, *110*, 3690–3692.

(51) Shokhirev, N. V.; Walker, F. A. Analysis of the Temperature Dependence of the ^{1}H Contact Shifts in Low-Spin Fe(III) Model Hemes and Heme Proteins: Explanation of "Curie" and "Anti-Curie" Behavior within the Same Molecule. *J. Phys. Chem.* **1995**, *99*, 17795–17804.

(52) Karlin, K. D.; Tyeklár, Z.; Farooq, A.; Jacobson, R. R.; Sinn, E.; Lee, D. W.; Bradshaw, J. E.; Wilson, L. J. Peroxide (O_2^{2-}) as a bridging ligand for copper(II): Strong exchange coupling in complexes derived from copper(I) and dioxygen. *Inorg. Chim. Acta* **1991**, *182*, 1–3.

(53) Kieber-Emmons, M. T.; Annaraj, J.; Seo, M.-S.; VanHeuvelen, K. M.; Tosha, T.; Kitagawa, T.; Brunold, T. C.; Nam, W.; Riordan, C. G. Identification of an "End-on" Nickel-Superoxo Adduct, $[Ni(tmc)(O_2)]^+$. *J. Am. Chem. Soc.* **2006**, *128*, 14230–14231.

(54) Irie, R.; Ito, Y.; Katsuki, T. Catalytic Epoxidation with Molecular Oxygen Using Nickel Complex. *Tetrahedron Lett.* **1991**, *32*, 6891–6894.

(55) Kinneary, J. F.; Albert, J. S.; Burrows, C. J. Mechanistic Studies of Alkene Epoxidation Catalyzed by Nickel(II) Cyclam Complexes. ^{18}O Labeling and Substituent Effects. *J. Am. Chem. Soc.* **1988**, *110*, 6124–6129.

(56) Nagataki, T.; Tachi, Y.; Itoh, S. Ni^{II}(TPA) as an efficient catalyst for alkane hydroxylation with *m*-CPBA. *Chem. Commun.* **2006**, 4016–4018.

(57) Stahl, S. S. Palladium Oxidase Catalysis: Selective Oxidation of Organic Chemicals by Direct Dioxygen-Coupled Turnover. *Angew. Chem., Int. Ed.* **2004**, *43*, 3400–3420.

AR700043N